Performance Investigation of DP-16QAM Ultra-wideband-Wavelength-Division Multiplexing Communication System: Optimum Power Consideration

Arwa A. Moosa[1,2], Raad Sami Fyath [3]

Authors affiliations:
1) Department of Laser and Optoelectronics Engineering, College of Engineering, Al-Nahrain University, Baghdad, Iraq.
2) Department of Networks Engineering, College of Engineering, Al- Iraqia University Baghdad, Iraq.
eng.arwa.amir@gmail.com

3) Department of Computer Engineering College of Engineering, Al-Nahrain University, Baghdad, Iraq.
rsfyath@yahoo.com

Paper History:

Received: 15th Jan. 2023

Revised: 26th Feb. 2023

Accepted: 19th March 2023

Abstract

Recently, there is increasing interest in using the 18 THz bandwidth offered by S+C+L band to increase the transmission capacity of fiber communication systems. This leads to the generation of ultra-wideband (UWB) wavelength-division multiplexing (WDM) optical communication systems. In these advanced systems, stimulated Raman scattering (SRS) causes a power transfer from high-frequency channels to low-frequency channels. This effect leads to an increase in the nonlinear interference (NLI) between the UWB-WDM channels. Power optimization techniques are required to balance transfer power between band channels, thus increasing the maximum transmission reach (MTR) along with increasing system capacity. In this paper, the transmission performance of S+C+L band system operating with dual-polarization 16-QAM signaling is investigated using enhanced Gaussian noise model. The transmitter and receiver for each DP channel use a 45^o-polarized laser and incorporate two identical configurations, one for x- and the other for y-state of polarization (SOP). The results are presented for two values of symbol rate, 40 and 80 GBaud, where the system carries 360 (=160+80+120) and 180 (=80+40+60) channels, respectively. The results revel that the MTR of both cases is equal to 12 100 km-spans when the channel lunch power equals to -4 and -2 dBm, respectively. This work also shows the effect of NLI components as a function of the number of spans, channel spacing, and channel launch power. The results show that the cross-phase modulation component of the NLI has high accumulated value with transmission distance, while the self-phase modulation component is almost constant.

Keywords: S+C+L WDM; Dual-polarization 16-QAM system; Stimulated Raman scattering; UWB-WDM system.

التحقيق في أداء DP-16QAM نظام اتصالات مضاعفة النطاق العريض للغاية - التي تعمل على تقسيم الطول الموجي: مع اعتبارات الطاقة المثلى

اروى عامر موسى ، رعد سامي فياض

الخلاصة:

في الآونة الأخيرة ، هناك اهتمام متزايد باستخدام عرض النطاق الترددي ١٨ THz الذي يوفره النطاق S+C+L لزيادة قدرة الإرسال لأنظمة الاتصالات البصرية وهذا يؤدي إلى توليد أنظمة اتصالات بصرية ذات نطاق عريض للغاية (UWB) لتقسيم الطول الموجي (WDM). في هذه الأنظمة المتقدمة ، يتسبب انتشار رامان المحفز (SRS) في نقل الطاقة من القنوات عالية التردد إلى القنوات منخفضة التردد. يؤدي هذا التأثير إلى زيادة التداخل غير الخطي (NLI) بين قنوات UWB-WDM. تقنيات تحسين القدرة مطلوبة لموازنة نقل القدرة بين قنوات هذا النطاق ، وبالتالي زيادة الوصول لأقصى أرسال (MTR) إلى جانب سعة النظام. في هذا البحث ، تم فحص أداء الإرسال لنطاق S+C+L، في نظام يعمل باستقطاب مزدوج QAM-١٦ باستخدام نموذج ضوضاء الغاوسي المحسن. يستخدم جهاز الإرسال والاستقبال لكل قناة DP ليزرًا مستقطبًا بزاوية ٤٥ درجة ويتضمن تكوينين متطابقين ، أحدهما لـ x والآخر لحالة y للاستقطاب (SOP). عرضت النتائج لقيمتين لمعدل الرمز ٤٠ و ٨٠ جيجابايت حيث يحمل النظام ٣٦٠ (= ١٦٠ + ٨٠ + ١٢٠) و ١٨٠ (= ٨٠ + ٤٠ + ٦٠) قناة على التوالي اظهرت النتائج أن MTR لكلتا الحالتين هو ١٢ امتداد (span) لالياف ذات طول ١٠٠ كم عندما تساوي القوة المغذية للقناة = -٤ و -٢ dBm ، على التوالي. يوضح هذا العمل أيضًا تأثير مكونات NLI كدالة لعدد الامتدادات، تباعد القنوات، والقوة المغذية للقناة. اظهرت النتائج أن

مكون NLI ذات تعديل الطور الانتقالي له قيمة متراكة عالية مع المسافة ، في حين أن مكون NLI ذات تعديل الطور الذاتي ثابت تقريبًا.

1. Introduction

Optical communication systems implemented with single-mode fibers (SMFs) can offer high data rate transmission over long haul distances [1], [2]. The SMF affects optical pulse propagation by its both linear and nonlinear effects [3], [4]. In ultra-wideband (UWB) transmission system, the nonlinear interchannel stimulated Raman scattering (SRS) and Kerr effect are the major limits of transmission data rates in optical communication systems [5], [6], and [7]. Note that although the channel power is low in optical communication system, the total power due to multichannel in WDM system is relatively large which makes the nonlinear fiber optics more effective in determining the system performance. These linear and nonlinear effects can be treated as an additive Gaussian noise (GN) [8], [9] and modeled by enhanced GN (EGN) approach for further high-order modulation considerations [10], [11] and [12]. Under this context, the linear effects can be reduced by using optical amplifiers [13] and digital signal processing (DSP), respectively [14]. On the other hand, the nonlinear effects can be minimized by selecting the optimal channel launch power which can significantly improve the signal quality [15], [16]. This consideration was investigated by GN model for C+L band system carries 660 channels with symbol rate R_s = 25 GBaud and 25.5 GHz channel spacing where it was found that the optimum power is -4 dBm for C band and -8.2 dBm for L band [17]. The GN model was also implemented for S+C+L band in [18] for 96 channels, 32 GBaud and 50 GHz channel spacing where it was found that -2.10, -1.99, and -1.43 dBm are the optimum power for S, C, and L subbands, respectively. The authors in [19] slashed S band into S1 and S2 subbands for further amplification control, and they found that the optimum power of 438-channel and 32 GBaud system are -0.4, -1.77, -6 and -6 dBm for S1, S2, C and L subbands, respectively. Note that the optimum powers in [17, 18 and 19] are different because each reference uses different number of channels, system rate, and modulation format. The NLI power of the GN model can be modified by EGN model which shows a high accurate results [10].

In this paper, the EGN model is used to investigate the optimal channel lunch power and transmission system performance of DP-16QAM S+C+L WDM systems when the channels occupy the whole band. The optimal power is chosen to minimize bit error rate (BER) performance of channels assuming equal channel launch power in all S+C+L band.

The rest of the paper is organized as follows. The system model is presented in Section 2. Section 3 provides system parameters and simulation results. Finally, Section 4 summarizes the main conclusions drawn from this study.

2. System Model

The S, C, and L subbands cover the 1460-1530, 1530-1565, and 1565-1625 nm spectrum range, respectively, as shown in Figure (1). The central wavelengths are 1495, 1547.5, and 1595, respectively. These parameters are important to design UWB-WDM systems where the WDM channels occupy the whole S+L+C band.

Figure (2a) presents a block diagram for the DP-S+C+L WDM system under investigation. The transmitter (receiver) side contains S-, C-, L- subband transmitters (receivers). The transmission link consists of multispan SMF with optical amplification scheme (OAS) is used at the end of each span to compensate its loss over the whole band. Figure (2b) illustrates the structure of a single span which contains a SMF section of length L_s followed by an OAS. Since no single optical amplifier (OA) is available practically over the whole band, individual S-, C-, and L-subband OAs are used. The gains of these OAs (G_S, G_C, and G_L) are equal to span length in km multiplied by the fiber loss evaluated at the central wavelength of the subband measured in dB/km. Thus, the total amplified spontaneous emission (ASE) noise is the accumulated noise added by the amplifiers. The group-velocity dispersion (GVD) and polarization dispersion of the SMF are compensated at the receive side for each channel using electronic dispersion compensation techniques. The configuration of DP-transmitter and receiver for each channel are illustrated in Figures (3a and b), respectively. Both configurations use 45^0-polrization laser to give equal power for both x- and y-polarizations. Both configurations use two identical versions, one for each state of polarization (SOP).

The transmission bandwidth of S+C+L system may exceed 15 THz toward 18 THz. This system is used to enlarge the transmission capacity [20]. This increase in band bandwidth enables an increase in number of transmission channels. Thus, the system is affected by SRS due its wide bandwidth and by Kerr effect due to increase in total lunch power. Optimal power consideration should be addressed carefully to reduce both effects. These two effects lead to nonlinear interference (NLI) which is characterized by self-phase modulation (SPM) and cross-phase modulation (XPM) components which are accumulated during signal propagation. The effect of four-wave mixing (FWM) component is negligible in WDM system operating with channel spacing Δf = 50 GHz (or more) when fiber dispersion is more than 2 ps/(km.nm) [21]. Such assumption is justified in this work since the dispersion of the fiber is > 2 ps/(km.nm) over all the S+C+L band. The dispersion compensation is achieved here at the end of the link using electronic compensation techniques. In such system, the channel power is affected by SRS which causes a power transfer from high-frequency to low-frequency channels, which influences the distribution of signal power by

$$\Delta P(z) = \sum_{q_{lower}}^{i} 4.3 C_r L_{eff} (P_{tot})_{lower} \, (B_{tot})_{lower} \quad \ldots..(1)$$

where q_{lower} is the maximum number of neighboring channels to the ith channel, $(P_{tot})_{lower}$ is the total channels launch power of the lower-band frequency, $(B_{tot})_{lower}$ is the total bandwidth of lower-band frequency, C_r is the Raman gain slope coefficient, and $L_{eff} = (1 - \exp(\alpha L))/\alpha$ is the effective length with L is the fiber length and α is the attenuation. Equation (1) is deduced from [22] after considering $>$ 15 THz bandwidth.

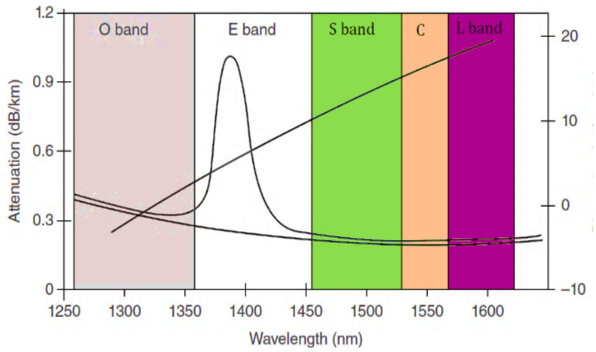

Figure (1): Different transmission bands over WDM systems [23].

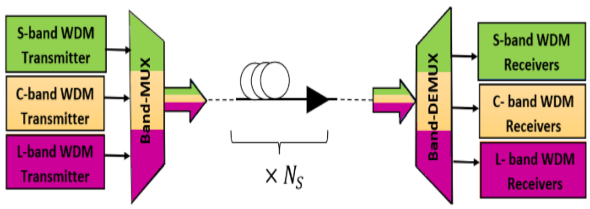

(a)

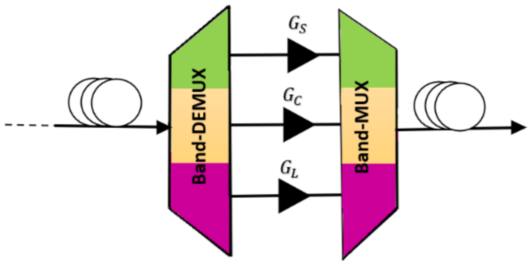

(b)

Figure (2): (a) Multispan loss compensated fiber for S+C+L UWB system, and **(b)** single span loss compensation.

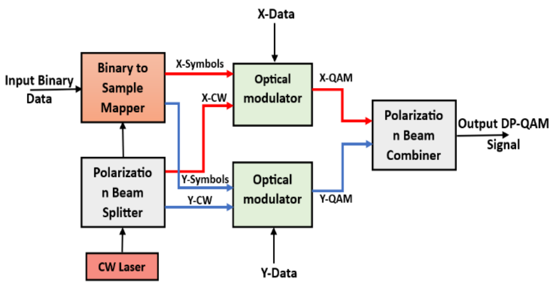

(a)

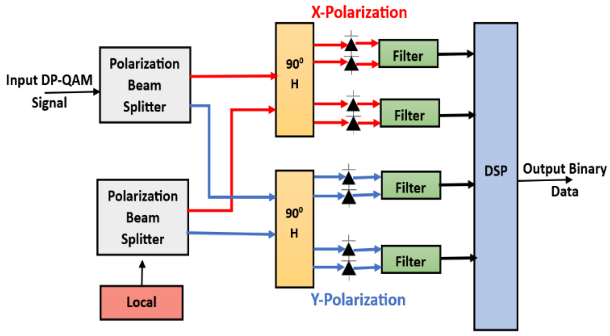

(b)

Figure (3): Block diagram configurations of DP-16QAM system(a) transmitter (b) receiver.

According to EGN model, the optical signal-to-noise ratio (OSNR) can be obtained as [24]

$$OSNR = \frac{P_r}{P_{ASE}+P_{NLI}} \quad \ldots(2)$$

where Pr is the received signal channel power and it is related to the input lunch power (Pi) by $Pr = Pi - \Delta P(z)$, P_{ASE} is the ASE noise power, and $P_{NLI} = \eta_n P_i^{\,3}$ is the nonlinear interference noise power caused by both SPM and XPM components. The total nonlinear coefficient η_n is taken as [25]

$$\eta_n \approx \sum_{j=1}^{N_s} \left[\frac{P_{i,j}}{P_i}\right]^2 \left[\eta_{SPM,i}(f_i)\, N_s^{\,\epsilon} + \eta_{XPM,j}(f_i)\right] \quad \ldots..(3)$$

where $\eta_{SPM,i}$, and $\eta_{XPM,j}$ are the nonlinear contributions of SPM and XPM, respectively (see Appendix A). Further, N_s is the number of spans used to construct the optical transmission link, P_i is the power of channel i lunched into the first span, $P_{i,j}$ is the power of channel i launched into jth span, f_i is the relative frequency of the channel of interest, and ϵ is a multispan coherent accumulation factor of SPM contribution which is given by [26]

$$\epsilon = \frac{3}{10} \log\left(1 + \frac{6}{L} \frac{L_{eff}}{\operatorname{asinh}((\pi^2/2)\beta_2 L_{eff} B_{ch}^2)}\right) \quad \ldots.(4)$$

In Equation (4), B_{ch} is the channel bandwidth, and β_2 is the fiber 2nd-order dispersion parameter.

In dB scale, the OSNR has a direct relationship with the signal-to-noise ratio SNR [27]

$$OSNR = SNR + 10 \times log_{10}\left(\frac{S_p B_e}{2B_0}\right) \quad \ldots.(5)$$

where S_p is number of the polarizations which is equal to 1 for single polarization and equal to 2 for dual polarization, B_e is the electrical signal bandwidth, and B_0 is the optical bandwidth. The ratio B_e/B_0 equals 0.5 (double-side optical band), and therefore, the electrical SNR can be obtained by

$$SNR = OSNR + 3dB \quad \ldots.(6)$$

The symbol error rate (SER) corresponding to 16-QAM format is given by [27]

$$SER_{16-QAM} = \frac{3}{2} erfc\left(\sqrt{\frac{SNR}{10}}\right) - \frac{7}{16} erfc^2\left(\sqrt{\frac{SNR}{10}}\right) \quad .....(7)$$

where erfc is the standard of the complementary error function. The BER is calculated from the SER by

$$BER = \frac{1}{4} SER \quad ....(8)$$

since each 16-QAM symbol has 4 bits ($log_2(16)$).

3. Results and Discussion

In this section, the performance of two DP-16QAM S+C+L WDM systems operating with 40 and 80 GBaud symbol rate R_s is investigated using Matlab program. The two systems have the following main parameters.

System I: R_s = 40 GBaud, Δf = 50 GHz, N_{ch} = 360 [S (160 channels) + C (80 channels) + L (120 channels)].

System II: R_s = 80 GBaud, Δf = 100 GHz, N_{ch} = 360 [S (80 channels) + C (40 channels) + L (60 channels)].

A 2 THz band space between S-C and C-L subbands are used to reduce the spectral overlapping between neighboring subbands. Further, it is assumed that all the WDM channels have the same symbol rate and modulation format. The parameter values used in the investigation are listed in Table (1) for three reference wavelengths corresponding to the central wavelengths of the S, C, and L subbands. Note that the fiber attenuation α at the reference wavelengths of S, C, and L subbands are 0.20, 0.17, and 0.18 dB/km, respectively. Therefore, the corresponding gains of the OAs inserted at the end of each 100 km span are G_S= 20 dB, G_C= 17 dB, and G_L= 18 dB.

Table (1): System parameters values.

Parameters	***Values***		
	S band	***C band***	***L band***
Reference Wavelength λ_{ref} (nm)	1495	1547.5	1595
Reference Frequency f_{ref} (THz)	200.8	193.8	188
Dispersion Coefficient D (ps/(nm.km))	13.700	17.000	19.700
Dispersion Slope S (ps/(nm^2.km))	0.060	0.060	0.050
Attenuation Coefficient α (dB/km)	0.200	0.170	0.180
Nonlinear Fiber Optics γ (1/W/km)	1.380	1.300	1.280
Raman gains slope C_r (1/W/km/THz)	0.028	0.027	0.026

Two metrics are given here to assign the performance of the investigated S+C+L WDM systems. Maximum transmission reach (MTR) which indicates the maximum number of spans that can be used to construct the transmission link while BER less than a specified threshold value (BER_{th}). In this work a threshold BER of 3.8× 10^{-3} is used which corresponds to 7% hard decision (HD) forward error correction (FEC) code [28]. BER here is that of the highest frequency channel since it is expected it offers the highest BER among the whole channels due to the influence of SRS effect.

It is worth to mention here that, MTR depends on channel lunch power P_{ch}. The optimum channel lunch power $(P_{ch})_{opt}$ which gives minimum received BER depends of number of link spans. The $(P_{ch})_{opt}$ describes the transmitter channel laser power in both SOPs which gives minimum total BER due to both SOPs. Figures ٤ (a&b) show BER versus channel launch power for N_s = 1, 5, and 10 spans and assuming R_s = 40 and 80 GBaud, respectively. The two values of R_s give almost the same BER results but with different channel lunch power. The 40 GBaud-system needs lower optimum power $(P_{ch})_{opt}$ to set the minimum BER (BER_{min}) due to its higher NLI that is caused by the 360 channels in comparison with the 180 channels of System II. The optimum lunch power is about -5 dBm for System I (Δf = 50 GHz and 360 channels) in comparison with -2 dBm for System II (Δf = 100 GHz and 80 channels). Note that $(P_{ch})_{opt}$ is almost independent on number of spans as shown in Table (2). Investigating the results in this table reveals that the optimum channel power is not affected by number of spans. In contrast, the BER increases with increasing number of spans.

It should be noted that the results obtained is related to the highest relative frequency in S subband because it loses the highest ΔP power by SRS effect. Table (2) shows a performance compression between the two different R_s values.

The variation of maximum transmission reach MTR with lunch power is depicted in Figure (٥) for both systems. The results show that the highest value of MTR offered by both systems = 12 spans and this occurs when P_{ch} = -4 and -2 dBm for System I and II, respectively.

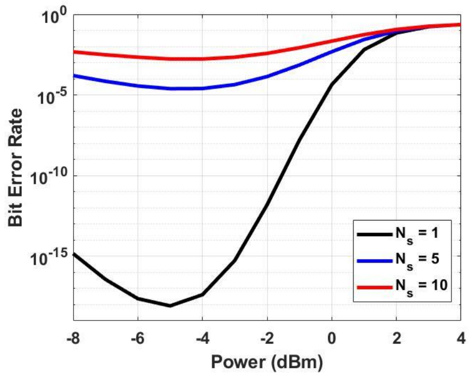

(a)

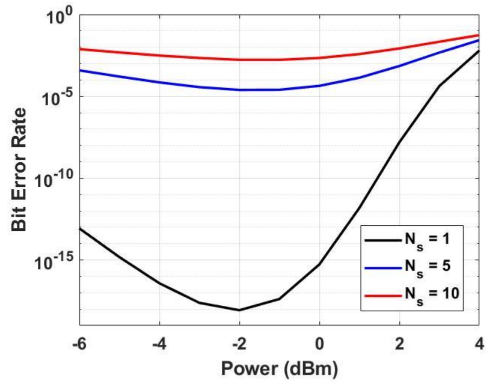

(b)

Figure (4): Variation of BER of DP-16 QAM S+C+L WDM system with lunched channel lunch power when (a) R_s =40 Gbaud and $\Delta f = 50\ GHz$, (b) R_s = 80 GBaud and $\Delta f = 100\ GHz$.

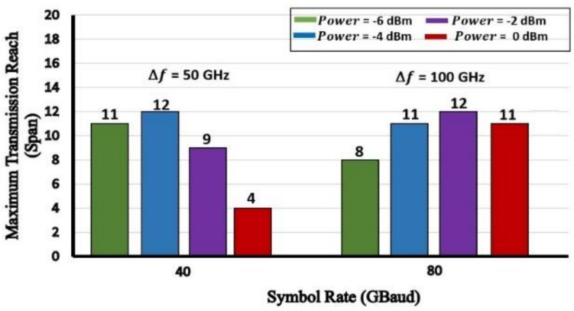

Figure (5): Number of maximum reach spans for DP-16QAM S+C+L WDM system operating with R_s = 40 and 80 GBaud for four values of channel lunch power.

The difference in results between R_s = 40 and 80 GBaud systems is due to increase of NLI level with the total channels launch power. Both XPM and SPM components of NLI limit the information capacity of optical fibers. This is due to the power fluctuations coming from the effect of the powers of other channels in case of XPM or from effect of its own power in case of SPM. Note that although SPM and XPM cause phase fluctuations, the presence of fiber dispersion introduced phase-to-intensity conversion.

The total NLI along with its XPM and SPM components are presented in Figures (6) and (7) as a function of number of spans N_s assuming P_{ch} = -4 and -2 dBm, respectively. Each figure contains three parts, a-c, corresponding to calculating these effects at relative frequencies f_{rel} of -9, 0, and +9 THz, respectively. The relative frequency denotes the deviation from the central frequency (1542.5 THz) of the S+C+L band. The results show that SPM component is almost independent of N_s because its value is accumulated by the multispan coherent accumulation factor ϵ which equals 0.1340, 0.1478, and 0.1579 for S, C and L subbands, respectively. However, the values of XPM component and total NLI increase with increasing the number of spans.

Table (2): Variation of optimum launch power and $\boldsymbol{BER_{min}}$ with number of spans.

40 GBaud		
Number of spans	***Optimum power (dBm)***	***BER***
1	*-5*	8.5×10^{-19}
5	*-4*	2.5×10^{-5}
10	*-4*	1.7×10^{-3}
80 GBaud		
Number of spans	***Optimum power (dBm)***	***BER***
1	*-2*	8.6×10^{-19}
5	*-2*	2.5×10^{-5}
10	*-2*	1.7×10^{-3}

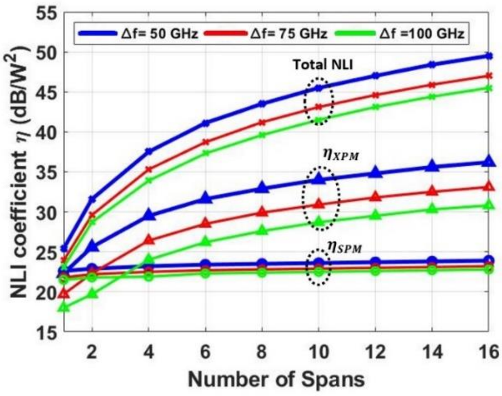

(a)

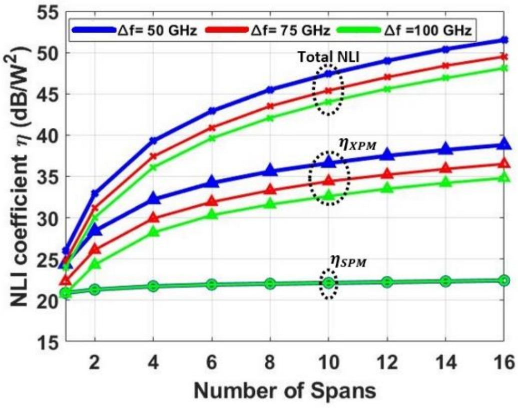

(b)

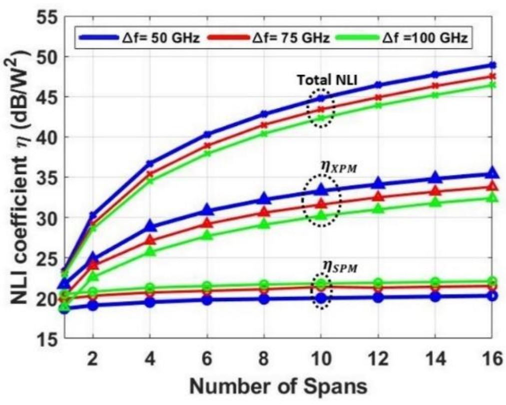

(c)

Figure (6): Variation of total and components, NLI, η_{XPM} and η_{SPM}, for DP-16QAM S+C+L system with -4 dBm channel lunch power of f_{rel} equal to (a) -9 THz, (b) 0 THz, and (c) +9 THz.

In both systems, reducing channel spacing causes to a reduction in the total NLI since it reduces the number of WDM channels. Designing System I with -4 dBm and Δf = 50 GHz yields total NLI of 23.4, 42.8, and 48.9 dB/W^2 for the +9 THz channel and 25.4, 43.5, and 49.5 dB/W² for the -9 THz when N_s = 1, 8, and 16, respectively.

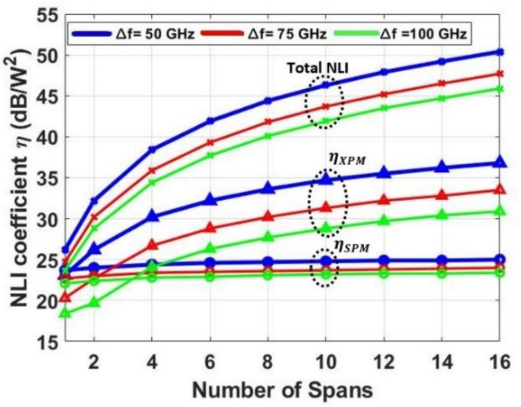

(a)

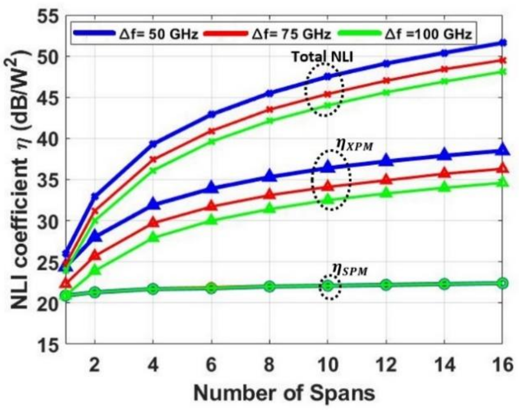

(b)

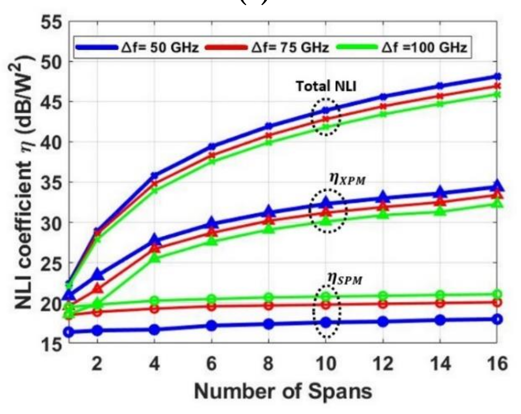

(c)

Figure (7): Variation of total and components, NLI, η_{XPM} and η_{SPM}, for DP-16QAM S+C+L system with -2 dBm channel lunch power of f_{rel} equal to (a) -9 THz, (b) 0 THz, and (c) +9 THz.

Increasing the P_{ch} to -2 dBm yields total NLI of 22.4, 41.9, and 48.1 dB/W^2 for the +9 THz channel and 26.2, 44.4, and 50.4 5 dB/W² for the -9 THz when N_s = 1, 8, and 16, respectively. When the same system is considered with P_{ch}= -4 dBm and $\Delta f = 100\ GHz$, the total NLI of +9 THz (-9 THz) is 22.9 (23.1), 37.9 (37.3), and 46.4 (45.5) dB/W^2 for N_s = 1, 6, and 16 respectively. This is due to lower number of channels in the system (180 channels) compared with 360 for $\Delta f = 50\ GHz$. Reducing the power from -2 dBm to -4 dBm causes a reduction in power transfer between the edge channel where the total NLI changes from 26.2 dB/W^2 for +9 THz and 22.4 dB/W^2 for -9 THz to 25.4 dB/W^2 for +9 THz and 23.4 dB/W^2 for -9 THz when using 1 span and $\Delta f = 50\ GHz$. Using different powers (i.e., -4 and -2 dBm) gives identical results for the central channel (f_{rel} = 0THz) since the effect of net SRS-transferred power is neglected at this frequency according to the EGN model.

4. Conclusions

The transmission of a UWB-WDM system needs careful consideration due to its high NLI caused by SRS and Kerr effects. Optimizing channel launch power is very useful to reduce the NLI effect. Using DP-16QAM S+C+L system with R_s = 40 GBaud and Δf= 50 GHz shows an optimum power of -4 dBm for multispan link and -5 dBm for single-span link. However, increasing R_s to 80 GBaud with Δf= 100 GHz shows an optimum power of -2 dBm for multi- and single-span links. Using 40 GBaud system with P_{ch} = -4 dBm yields 12-span MTR assuming 100 km SMF per span. In other hand, the 80 GBaud system can reach the same MTR value but with P_{ch} = -2 dBm. The results indicate that the XPM component of the NLI has high accumulated value with distance, while the SPM component of the NLI is almost constant.

Appendix A
Summary of the Enhanced Gaussian Noise (EGN) Model

For DP-16 QAM S+C+L multi-span system, the nonlinear interference (NLI) noise can be considered as additive Gaussian noise and resolved by the EGN assumption model. NLI noise is contributed by two factors, SPM and XPM, as shown in Equation (3). The SPM and XPM contributions are given by [29]

$$\eta_{SPM}(f_i) \approx \frac{4}{9}\frac{\gamma^2}{B_i^2}\frac{\pi}{\phi_i\,\bar{\alpha}\,(2\alpha+\bar{\alpha})}\cdot\left[\frac{T_i-\alpha^2}{\alpha}\operatorname{asinh}\left(\frac{\phi_i\,B_i^2}{\pi\alpha}\right)+\frac{A^2-T_i}{A}\operatorname{asinh}\left(\frac{\phi_i\,B_i^2}{\pi A}\right)\right] \quad \ldots\ldots(8)$$

where $\phi_i = \frac{3}{2}\pi^2(\beta_2 + 2\pi\beta_3 f_i),\ A = \alpha + \bar{\alpha}\ \ and\ T_i = (\alpha + \bar{\alpha} - P_{tot}C_r\, f_i)^2$

$$\eta_{XPM}(f_i) \approx \frac{32}{27}\sum_{k=1\ k\neq i}^{N_{ch}}\left(\frac{P_k}{P_i}\right)^2\frac{\gamma^2}{B_k}\left\{\frac{n+\frac{5}{6}\Phi}{\phi_{i,k}\bar{\alpha}\,(2\alpha+\bar{\alpha})}\cdot\left[\frac{T_k-\alpha^2}{\alpha}\operatorname{atan}\left(\frac{\phi_{i,k}B_i}{\alpha}\right)+\frac{A^2-T_k}{A}\operatorname{atan}\left(\frac{\phi_{i,k}B_i}{A}\right)\right]+\frac{5}{3}\frac{\Phi\pi\breve{N}T_k}{|\phi|B_k^2\alpha^2A^2}\left[(2|\Delta f|-B_k)\log\left(\frac{2|\Delta f|-B_k}{2|\Delta f|+B_k}\right)+2B_k\right]\right\} \quad \ldots..(9)$$

The parameter $\breve{N}$ in Equation (9) depends on the number of spans N_s

$$N^{\sim} = \begin{cases} 0, & if\ N_s = 1 \\ N_s, & otherwise \end{cases} \quad ....(10)$$

kurtosis parameter (i.e., the modulation factor Φ) is defined as in [10] $\Phi = (E\{|x|^4\}/E^2\{|x|^2\}) - 2$, where x denotes the data symbol and E is the expectation operator. The modulation factor Φ is equal to -0.68 for 16-QAM. Further, $T_k = (\alpha + \bar{\alpha} - P_{tot} C_r f_k)^2$ and $\phi_{i,k} = 2\pi^2 (f_k - f_i)(\beta_2 + 2\pi\beta_3 f_i)$. where, f_i and f_k are the relative frequencies of the interest ith channel and interfering kth channel, respectively. To simplify the calculations, the attenuation parameter α is assumed equals to the average attenuation $\bar{\alpha}$. Note that ϕ_i and $\phi_{i,k}$ corresponding to SPM at frequency f_i and XPM between the two frequencies i and k, respectively.

4. References

[1] H. F. Benjamin J. Puttnam, Ruben S. Luís, Georg Rademacher, Yoshinari Awaji, "Investigation of Long-Haul S- , C- + L-Band Transmission," in 2022 Optical Fiber Communication (OFC) Conference, 2022, pp. 1–3.

[2] C. R. Kobayashi, Takayuki, Cho, Junho, Lamponi, Marco, De Valicourt, Guilhem, Doerr, "Coherent Optical Transceivers Scaling and Integration Challenges," Proceedings of the IEEE, vol. 110, no. 11, pp. 1679–1698, 2022, doi: 10.1109/jproc.2022.3206268.

[3] D. Semrau, "Modeling of Fiber Nonlinearity in Wideband Transmission," in 2022 Optical Fiber Communication (OFC) Conference, Optica Publishing, 2022, pp. 6–8. doi: 10.1364/ofc.2022.w3c.6.

[4] X. Ming, Hao, Chen, Xinyu, Fang and F. Zhang, Lei, Li, Chenjia, Zhang, "Ultralow Complexity Long Short-Term Memory Network for Fiber Nonlinearity Mitigation in Coherent Optical Communication Systems," J Journal of Lightwave Technology, vol. 40, no. 8, pp. 2427–2434, 2022, doi: 10.1109/JLT.2022.3141404.

[5] G. C. Salma Escobar Landero, Ivan Fernandez de Jauregui Ruiz, Alessio Ferrari, Dylan Le Gac, Yann Frignac, "Link Power Optimization for S+C+L Multi-band WDM Coherent Transmission Systems," in 2022 Optical Fiber Communication (OFC) Conference, Optica Publishing, 2022, pp. 1–3. doi: 10.1364/ofc.2022.w4i.5.

[6] S. de Koster, Pascal, Koch, Jonas, Schulz, Olaf, Pachnicke, Stephan, and Wahls, "Experimental Validation of Nonlinear Fourier Transform-Based Kerr-Nonlinearity Identification Over A 1600 Km SSMF Link," in 2022 Optical Fiber Communication (OFC) Conference, 2022, pp. 1–3. doi: 10.1364/ofc.2022.w2a.39.

[7] H. Rabbani, H. Hosseinianfar, H. Rabbani, and M. Brandt-Pearce, "Analysis of Nonlinear Fiber Kerr Effects for Arbitrary Modulation Formats," Journal of Lightwave Technology, vol. 41, no. 1, pp. 96–104, 2022, doi: 10.1109/JLT.2022.3213182.

[8] L. R. Amirabadi, Mohammad Ali, Kahaei, Mohammad Hossein, Nezamalhosseini, and S. Alireza, Chen, "Optimal Power Allocation In Nonlinear MDM-WDM Systems Using Gaussian Noise Model," IET Optoelectronics, vol. 16, no. 3, pp. 133–148, 2022, doi: 10.1049/ote2.12064.

[9] J. Zhang, Chengliang, Liu, Xiang, Li and J. Zhang, Anxu, Liu, Hao, Feng, Lipeng, Lv, Kai, Liao, Shenghui, Chang, Zeshan, Zhang, "Optical Layer Impairments and Their Mitigation in C+L+S+E+O Multi-Band Optical Networks With G.652 and Loss-Minimized G.654 Fibers," Journal of Lightwave Technology, vol. 40, no. 11, pp. 3415–3424, 2022, doi: 10.1109/JLT.2022.3166652.

[10] A. Soleimanzade and M. Ardakani, "EGN-Based Optimization of the APSK Constellations for the Non-Linear Fiber Channel Based on the Symbol-Wise Mutual Information," Journal of Lightwave Technology, vol. 40, no. 7, pp. 1937–1952, 2022, doi: 10.1109/JLT.2021.3132863.

[11] A. J. Lowery and L. B. Y. Du, "XPM Efficiency Versus Symbol Rate," Journal of Lightwave Technology, vol. 40, no. 9, pp. 2850–2861, 2022, doi: 10.1109/JLT.2022.3148414.

[12] H. Rabbani, H. Hossienianfar, and M. Brandt-Pearce, "An Enhanced Analytical Model of Nonlinear Fiber Effects for Four-Dimensional Symmetric Modulation Formats," Journal of Lightwave Technology, vol. 40, no. 16, pp. 5567–5574, 2022, doi: 10.1109/JLT.2022.3183162.

[13] M. F. Mikhailov, Vitaly, Luo, Jiawei, Inniss, Daryl, Yan and D. J. Sun, Yingzhi, Puc, Gabriel S., Windeler, Robert S., Westbrook, Paul S., Dulashko, Yuriy, Digiovanni, "Amplified Transmission Beyond C- and L- Bands: Bismuth Doped Fiber Amplifier for O-Band Transmission," Journal of Lightwave Technology, vol. 40, no. 10, pp. 3255–3262, 2022, doi: 10.1109/JLT.2022.3169172.

[14] L. Rapp and M. Eiselt, "Optical Amplifiers for Multi-Band Optical Transmission Systems," Journal of Lightwave Technology, vol. 40, no. 6, pp. 1579–1589, 2022, doi: 10.1109/JLT.2021.3120944.

[15] T. Liu, Zheng, Xu, Tianhua, Jin, Cenqin, Xu, Tongyang, Tan, Mingming, Zhao, Jian, Liu, "Analytical Optimization of Wideband Nonlinear Optical Fiber Communication Systems," Optics Express, vol. 30, no. 7, p. 11345, 2022, doi: 10.1364/oe.453307.

[16] D. W. Roberts, Ian, Kahn, Joseph M., Harley, JamesmBoertjes, "Channel Power Optimization of WDM Systems Following Gaussian Noise Nonlinearity Model in Presence of Stimulated Raman Scattering," Journal of Lightwave Technology, vol. 35, no. 23, pp. 5237–5249, 2017, doi: 10.1109/JLT.2017.2771719.

[17] H. Buglia, E. Sillekens, A. Vasylchenkova, P. Bayvel, and L. Galdino, "On The Impact of Launch Power Optimization And Transceiver Noise on The Performance of Ultra-Wideband Transmission Systems [Invited]," Journal of Optical Communications and Networking, vol. 14,

no. 5, pp. B11–B21, 2022, doi: 10.1364/JOCN.450726.

[18] V. Correia, Bruno, Sadeghi, Rasoul, Virgillito, Emanuele, Napoli, Antonio, Costa, Nelson, Pedro, Joao, Curri, “Networking Performance of Power Optimized C+L+S Multiband Transmission,” in 2020 IEEE Global Communications Conference, GLOBECOM 2020 - Proceedings, 2020, pp. 2–7. doi: 10.1109/GLOBECOM42002.2020.9322068.

[19] D. Uzunidis, C. Matrakidis, E. Kosmatos, A. Stavdas, and A. Lord, “On The Benefits of Power Optimization in The S, C and L-Band Optical Transmission Systems,” Computer Networks, vol. 211, p. 108958, 2022, doi: 10.1016/j.comnet.2022.108958.

[20] H. Luo, J. Lu, Z. Huang, C. Yu, and C. Lu, “Optimization Strategy of Power Control For C+L+S Band Transmission Using A Simulated Annealing Algorithm,” Optics Express, vol. 30, no. 1, p. 664, 2022, doi: 10.1364/oe.439635.

[21] G. P. Agrawal, "Fiber-Optic Communication Systems". Wiley, 5th Edition, 2021.

[22] S. Okamoto et al., “A Study on the Effect of Ultra-Wide Band WDM on Optical Transmission Systems,” Journal of Optical Communications and Networking, vol. 38, no. 5, pp. 1061–1070, 2020, doi: 10.1109/JLT.2019.2962178.

[23] G. P. Agrawal, "Fiberoptic communication systems", 2021. doi: 10.1080/09500349314550971.

[24] A. Souza, N. Costa, J. Pedro, and J. Pires, “Benefits of Counterpropagating Raman Amplification for Multiband Optical Networks,” Journal of Optical Communications and Networking, vol. 14, no. 7, p. 562, 2022, doi: 10.1364/jocn.456582.

[25] D. Semrau, E. Sillekens, P. Bayvel, and R. I. Killey, “Modeling and Mitigation of Fiber Nonlinearity in Wideband Optical Signal Transmission [Invited],” Journal of Optical Communications and Networking, vol. 12, no. 6, pp. C68–C76, 2020, doi: 10.1364/JOCN.382267.

[26] P. Poggiolini, “The GN Model Of Non-Linear Propagation in Uncompensated Coherent Optical Systems,” Journal of Lightwave Technology,, vol. 30, no. 24, pp. 3857–3879, 2012, doi: 10.1109/JLT.2012.2217729.

[27] A. Dissertation, “Development and Design a Compensation Method for Fiber Impairment in Ultra-High Speed Dense Wavelength Division Multiplexing (DWDM) Transmission System Based on Artificial Neural Network”, PhD Thesis, University of Babylon, 2021.

[28] H. K. Chan, David W.U., Wu, Xiong, Zhang, Zunyue, Lu, Chao Lau, Alan Pak Tao, Tsang, “Ultra-Wide Free-Spectral-Range Silicon Microring Modulator for High Capacity WDM,” Journal of Lightwave Technology, vol. 40, no. 24, pp. 7848–7855, 2022, doi: 10.1109/JLT.2022.3208745.

[29] E. Semrau, Daniel, Sillekens and P. Killey, Robert I., Bayvel, “A Modulation Format Correction Formula for the Gaussian Noise Model in the Presence of Inter-Channel Stimulated Raman Scattering,” Journal of Lightwave Technology, vol. 37, no. 19, pp. 5122–5131, 2019, doi: 10.1109/JLT.2019.2929461.